Shahrood University of Technology

Journal of Mining and Environment (JME)

Journal homepage: www.jme.shahroodut.ac.ir

Iranian Society of Mining Engineering (IRSME)

Determination of Mechanical Parameters of Anthracite Coal using Flying Squirrel Search Algorithm with Timber Load and Displacement Data

Myong Nam Sin[1], Un Chol Han[2]*, Hyon Hyok Ri[1], and Sung Il Jon[3]

1. Faculty of Mining Engineering, Kim Chaek University of Technology, Pyongyang, Democratic People's Republic of Korea
2. School of Science and Engineering, Kim Chaek University of Technology, Pyongyang, Democratic People's Republic of Korea
3. Department of Applied Mathematics, Kim Chaek University of Technology, Pyongyang, Democratic People's Republic of Korea

Article Info

Received 22 March 2023
Received in Revised form 21 April 2023
Accepted 4 May 2023
Published online 4 May 2023

DOI:10.22044/jme.2023.12869.2335

Keywords

SSA
Displacement back analysis
Neural network
Time-dependent mechanical parameter

Abstract

Anthracite coal seam of Democratic People's Republic of Korea was broken into particles to be soft due to geological tectonic actions through several stages in the Mesozoic era. Because the folds and faults have excessively developed and the shape of coal seam is very complicated, it is impossible to extract the anthracite coal by longwall mining system, and coal has been mainly mined by entry caving mining system. The aim of this work is to assess effectiveness of new combination of flying squirrel search algorithm (SSA) and artificial neural-network (ANN) for back-analysis of time-depending mechanical parameters of anthracite coal based on timber loads and displacements measured in the coal face entry. The case study deals with a coal face entry in Sinchang Coal Mine located in the Unsan County, South Pyongan Province, DPR Korea. To verify the good performance of new combination of the SSA and ANN, the comparison studies between proposed back-analysis method and other methods with the same purpose, are conducted using data measured in coal face entry. The mean absolute error (MAE) of weighted error norm of ANN-SSA is relatively smaller in comparison with other methods, which is 2.49. The new back-analysis is the good method to determine the suitable time-dependent mechanical parameters of anthracite coal surrounding the entry in very soft coal seam.

1. Introduction

The coal mechanical parameters and the initial stress have predominant influences on the stability of the surrounding coal of an entry in the coal seam. However, in practice, it is very difficult to determine the values of the time-dependent soft coal mass parameters. To obtain these values of the time-dependent soft coal mass parameters based on very limited amounts of measured data, back-analysis is the most commonly used approach worldwide. Field measurement data may include displacements [1–4], strains, and stresses [5, 6].

Because the displacements of a rock mass can be measured easily and reliably, back-analysis based on displacements has long been an active topic of research. Some important studies are summarized below.

Ghorbani and Sharifzadeh [7] have proposed the displacement based direct back-analysis using univariate optimization algorithm by which geo-mechanical properties of rocks, stress ratio, and joints parameters are identified. Zhang *et al*. [8] have determined the modulus of elasticity and the horizontal *in situ* stress perpendicular to the axis line of the opening for the Zhanghewan Pumped Storage Power Station in China using iterative algorithms such as the direct search technique and the damped least squares technique in combination with the three-dimensional finite-element pattern technique for displacement back-analysis.

The values for the modulus of elasticity, the poisson's ratio, and the six components of the initial stress levels of the ground for a tunnel have been identified using the three-dimensional finite-

✉ *Corresponding author: huch8272@star-co.net.kp (U.Ch. Han)*

element method and the secant method by Hisatake and Hieda [9]. Han *et al*. [2] proposed a displacement back-analysis based on grey vehulst model, and Yang *et al*. [10] have estimated the stress increment and viscoelastic parameters of a surrounding rock mass for a tunnel using a three-element model for displacement back analysis.

In a departure from the studies described above, Liang *et al*. [11] have proposed a new back analysis method based on a fuzzy back-propagation neural network (BPNN), and have used this method to identify the mechanical parameters and initial stresses of the surrounding rock for underground engineering projects based on measured displacements. Feng *et al*. [12] have suggested the new displacement back-analysis to identify mechanical geo-material parameters based on hybrid intelligent methodology, which is an integration of evolutionary support vector machines (SVMs), numerical analysis, and genetic algorithm. Also Feng *et al*. [13] have proposed the approach for estimating the mechanical rock mass parameters relating to the three gorges project permanent ship lock using an intelligent displacement back-analysis method, which is a combination of a neural network, an evolutionary calculation, and numerical analysis techniques. Yu *et al*. [14] have proposed an intelligent method for the effective displacement back-analysis of earth-rockfill dams by combining neural networks and evolutionary calculation, which can employ neural networks, with optimal architecture trained by the evolutionary calculation and Vogl's algorithm, instead of the time-consuming finite element analysis.

Zhang *et al*. [15] have suggested the displacement-based back-analysis method for the determination of rock mass modulus and the horizontal *in situ* stress perpendicular to the axis line of the tunnel excavation in hard and intact rock masses, whose principle is a best-fit solution of back-analysis by comparing the measured displacements near a tunnel face during excavation with those calculated using a three-dimensional finite element method. Yazdani *et al*. [16] have identified the geo-mechanical properties of rocks, stress ratios and joint parameters of the Siah Bisheh powerhouse cavern in Iran using a univariate optimization algorithm and the Fast Lagrangian Analysis of Continua (FLAC) software package for displacement of back-analysis. Sharifzadeh *et al*. [17] have estimated the rock properties and initial stress ratio for the Shibli twin tunnels in Iran based on displacement monitoring results using a univariate optimization algorithm and the FLAC. Besides, Gao and Ge [18] have proposed a new back-analysis method based on the novel evolutionary neural network that can be used to simultaneously determine the material parameters and the initial stress, which applies the immunized evolutionary programming to improve the back-analysis performance. Yu *et a1*. [19] have proposed a back-propagation neural-network-based displacement back-analysis method for the identification of the geo-mechanical parameters of the Yonglang landslide in China based on loading tests on a loading-test pile conducted to measure the displacements and moments. Gao *et al*. [20] have proposed the new neural network based on black hole algorithm to overcome the shortcomings of the traditional neural networks. Luo *et al*. [21] have proposed the displacement back-analysis method to calculate the rock mass parameters, double parameters analyzed by using the golden section method. Mohamad *et al*. [22] and Rezaei [23] have proposed the new combination and application of intelligent techniques including adaptive neuro-fuzzy inference system (ANFIS), genetic algorithm (GA), and particle swarm optimization (PSO) to predict rock UCS based on indirect test methods. Rezaei *et al*. [24,25] and Wang and Rezaei [26] have used ANFIS-DE (differential evolution), ANFIS-FA (firefly algorithm), BPNN, radial basis function network (RBFNN) and multiple linear regression (MLR) techniques to estimate elastic modulus of intact rocks based on laboratory tests.

From an analysis of previous studies, the following conclusions can be drawn. The basic methods used in the most studies have been numerical simulation methods and optimization algorithms. In these methods, numerical simulations are used to compute the displacements of the surrounding rock based on certain assumed values of the mechanical parameters and the initial stress. Then by optimizing the error between the computed displacements and the measured displacements via an optimization algorithm, the initially assumed values can be corrected into the real values. Therefore, this type of back-analysis is called optimization back-analysis. However, there are a few papers that deal with back-analysis method based on timber load and displacement measured in the entry in case the rock pressure and displacement of the entry increase continuously owing to the coal softening with time in very soft coal such as anthracite coal.

The aim of this work is to assess the effectiveness of new combination of flying

squirrel search algorithm (SSA) and BPNN for back-analysis of time-depending mechanical parameters of anthracite coal based on timber loads and displacements measured in the coal face entry. For doing this, we propose the methodology to estimate the time-depending mechanical parameters of coal by new combination of ANN and SSA.

2. Engineering Background and Field Measurements

2.1. Field condition and measuring method

The case study deals with a coal face entry in Sinchang Coal Mine located in Unsan County, South Pyongan Province, DPR Korea. Anthracite coal seams were broken into particles due to geological tectonic actions through several stages in the Mesozoic era. Because the folds and fault are excessively developed and the shape of coal seam is very complicated, it is impossible to extract the anthracite coal by longwall mining system and coal is mainly mined by entry caving mining system. The coal faces where the load acting to the support and convergence of entry were measured are buried in 200 m deep from the surface. The driving cross-section of the entries is about 5 m^2 and finished cross-section 4 m^2. The average thickness of anthracite coal seam is 5.5 m and it has an gentle incline of 12°. Anthracite coal has been extracted by various kinds of entry caving coal mining systems. The principle layout of the enry caving mining system appied in this coal mine is shown in Figure 1.

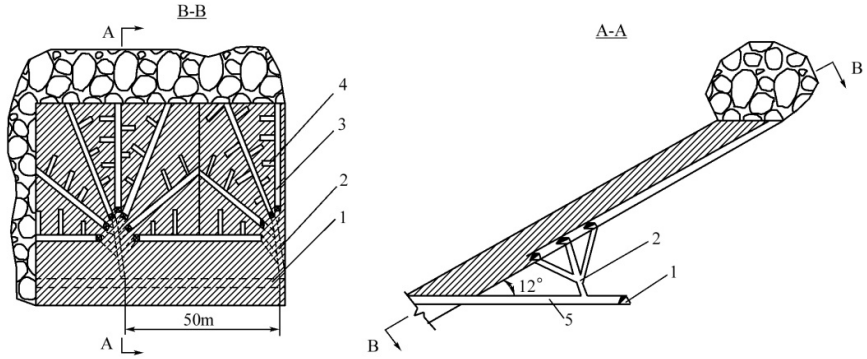

Figure 1. Principle layout of enry caving mining system:
1-level haulage roadway, 2-raise, 3-entry or diagonal entry, 4-side cavern for caving, 5-crosscut

The length of entry in this coal face is about 25~30 m, and its maintenance period is about 30 days. Wooden timbers are installed in the entry, whose diameter is about 18 cm and installation interval is 0.6~0.7 m. The measuring points are 5 m away from a scraper conveyer head part and 30 m to a conveyer end part. We measuered vertical and horizontal load acting to the beam and legs of the timber, vertical convergence between the crown and floor of entry and horizontal one between both of sidewalls of entry. Vertical load was measured with installation of 200 kN class loadcell and horizontal load by 150 kN class load cell. The measuring points in the coal between two timbers were installed to measure vertical and horizontal convergence. The convergences were measured by means of a laser distance meter, whose mark is DIST^{TM}A2.

Considering the installing condition of the loadcell, it was fixed between the post set up in the middle of timber beam and then vertical load acting to the timber was measured. After the lagging of 15 cm in diameter was put into between the two legs of both of timber and coal wall, 150 kN class loadcell was installed between the lagging and timber leg to measure the horizontal load. The installing plan of loadcells to measure vertical and horizontal load acting to the timber is shown in Figure 2.

The measuring points were set up in the floor of entry and between the beams of timbers to measure the vertical convergence of the entry. The measuring points were set up in the coal wall between two legs of timbers to measure the horizontal convergence of the entry. The measuring points for surveying the convergence were established by drilling the holes 30 mm in diameter and 1.5 m long and driving steel bars into the holes. The layout of measuring points for surveying the convergence of entry is shown in Figure 3.

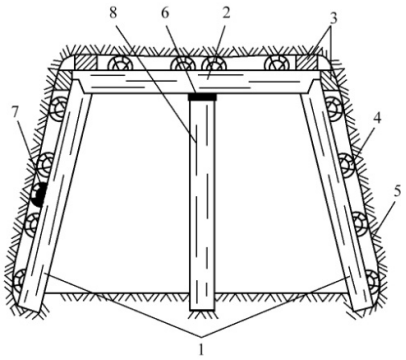

Figure 2. Installing plan of loadcells to measure vertical and horizontal load acting on timber 1-leg, 2-beam, 3-wedge, 4-lagging , 5-coal, 6-200 kN-class loadcell, 7-150 kN-class loadcell, 8-middle post.

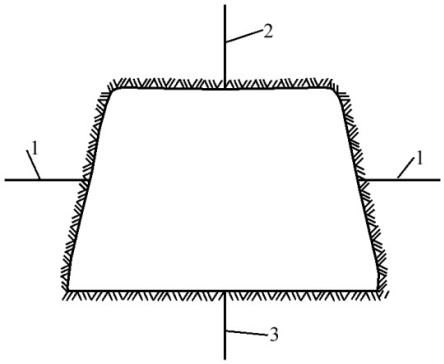

Figure 3. Layout of measuring points for surveying vertical and horizontal convergence of entry: 1-measuring point in the side walls, 2 and 3-measuring points in the roof and floor.

2.2. Measured data analysis

2.2.1. Analysis of loads acting on timber

After setting up loadcells and convergence measuring points, loads acting to the timber and convergence of the entry were simultaneously measured at 3 days intervals during 30 days. The time–dependent vertical and horizontal distribution load acting to the timber is shown in Figure 4.

As shown in Figure 4, we can find that rock pressure acting to the entry is unstable with the lapse of time and it continuously increases. Under the condition of knowing the vertical and horizontal distribution load, lateral pressure coefficient $\lambda = {}^{P_h}/_{P_v}$ (where P_v and P_h-vertical and horizontal distribution load, respectively) was determined in the anthracite coal seam where measurements were conducted, whose result is listed in Table 1.

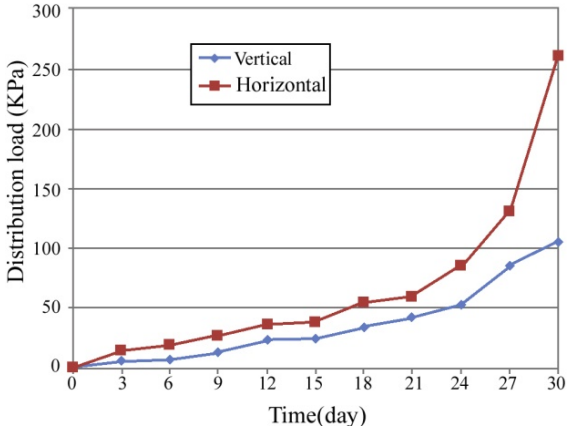

Figure 4. Change charateristics of vertical and horizontal distribution load acting to the timber depending on time.

Table 1. Change of lateral pressure coefficient depending on time.

Measured date (days)	Vertical distribution load (KPa)	Horizontal distribution load (KPa)	Lateral pressure coefficient
3	5.6	14.8	2.64
6	7.4	19.2	2.6
9	12.5	26.9	2.152
12	23.6	35.7	1.512
15	24.5	38.5	1.57
18	34.2	54.5	1.593
21	42.1	60.6	1.44
24	52.3	85.7	1.64
27	85.6	130.95	1.53
30	105.4	260.76	2.47
Average	39.32	72.76	1.914

Table 1 shows that the lateral pressure coefficients are changed along with time, their range is 1.44~2.64, and average value is about 2.

2.2.2. Analysis of convergence displacements of entry

The middle post starts to is driven into the floor of entry under the rock pressure two days after installing the measurement points. The reason is that coal is so soft that floor coal can't resist the timber legs driving. As the entry deformation was so large that it was nearly collapsed at near completion of measurement, convergences measured in 27 and 30 days were not exact. Therefore, the values are excepted from analysis and the vertical and horizontal convergence of the entry depending on time is shown in Figure 5, which is graphed by using rest measured values. As shown in Figure 5, we can find that the entry deformation is unstable with the lapse of time, and it continuously increases.

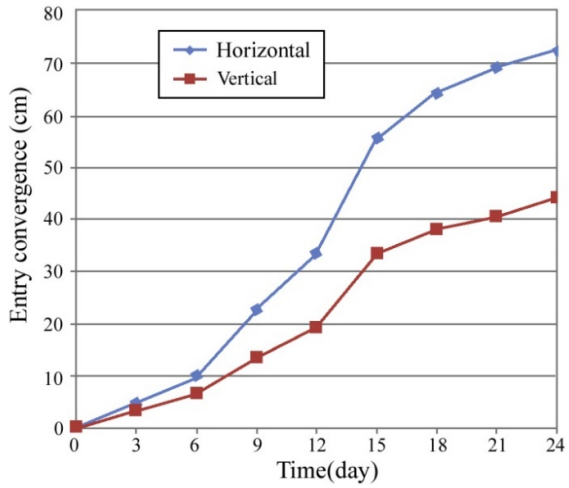

Figure 5. Change charateristics of vertical and horizontal convergence of entry in coal seam depending on time.

3. Methodology for predicting mechanical parameters of coal by back-analysis

3.1. Rock pressure characteristics of entry in anthracite coal seam

The reason why rock pressure of the entry driven in the anthracite coal seam is large is as follows according to field observation. In case the intact coal is extracted from anthracite coal seam, we can see severe rock pressure phenomena. The phenomenon that the entry deformation under the above condition becomes large can not be fully described. If a space in the coal seam that has been compressed due to complicated tectonic actions is formed, coal is in contact with air to swell, so the mechanical parameters of coal undergo a great change in the process. The cohesion and internal friction angle of charactering the coal strength and the elastic modulus of charactering the coal deformability become weak with the lapse of time, which is the process of coal swelling.

As shown in the above section, the increase of vertical and horizontal load acting to the timber with the lapse of time can be considered as plastic zone growth because the cohesion and internal friction angle of charactering the coal strength become weak along with time. It is very difficult to illustrate this process on an analytic basis but it can be easily analyzed by applying an intelligent back analysis method. The Mohr-Coulomb criterion is used in numerical simulation of coal failure process.

3.2. Back-analysis based on flying squirrel search algorithm (SSA)

Shown in Figure 6 is the flowchart for back-analyzing the mechanical parameters of anthracite coal by combining finite difference method (FDM) with neural network and SSA.

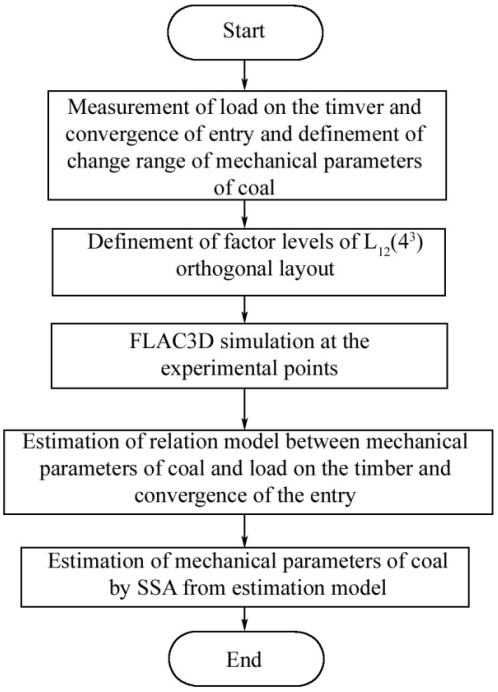

Figure 6. Back-analysis flowchart by combining FDM with ANN and SSA.

In order to back-analyze the mechanical parameters of coal according to the flowchart

shown in Figure 6, we should go through the following steps.

Firstly, in order to measure the vertical and horizontal load acting to the timber and vertical and horizontal convergence of the entry during drifting and coal mining, the measuring points are set up at the position some away from the driving face and the values are recorded that are measured at fixed time intervals until the entry suffers from severe mining effect.

Secondly, the ranges of the mechanical parameters of coal should be preliminarily selected based on measured data and engineering experiences.

After establishing the numerical model, various input values based on preliminarily-selected mechanical parameters are used to calculate the convergences of the entry and plastic zone size surrounding the entry. The output values from FLAC3D modelling approach the approximate range of measured results through repeated numerical simulation, so we can determine the ranges of mechanical parameters of rock mass to arrange the parameter combinations for the FDM.

Thirdly, based on the experimental factors and design levels as well as the basic principles of orthogonal experimental design, an orthogonal layout is used to arrange the parameter combinations for the FDM.

Fourthly, using above numerical simulation data weights and biases are determined by neural network to establish the database, which can be used by SSA.

Fifthly, the mechanical parameters are finally determined with measured time in a new combination of the neural network and SSA based on measured load and displacement.

3.3. Flying squirrel search algorithm (SSA)

In the recent years, Jain *et al*. [27] have proposed a new simple and powerful nature-inspired algorithm called squirrel search algorithm (SSA) for unconstrained numerical optimization problems. This algorithm simulates the dynamic foraging strategy of southern flying squirrels and their efficient way of gliding known as locomotion.

As the squirrel search method is one of swarm intelligent search methods, it has been estimated that its search efficiency is very high. The main idea of this method is as follows.

The swarm of squirrels is randomly located in the search space. Here, we suppose that squirrels are always on any trees. The feed that squirrels like most is hickory tree, which is defined as the best location (minimum fitness value) where a squirrel among the swarm takes. The tree that squirrel likes next is acorn tree and we consider it as a tree with the position that the order of fitness values among the swarm becomes greater from the second to the fourth. The positions of rest squirrels are on normal trees without feed. Squirrels on the acorn trees are going to the hickory trees. Squirrels on the normal trees are going to the acorn trees or hickory trees. However, presences of predator make them cautious and are forced them to use small random walk to search a nearby hiding location. Predator to squirrels can appear with constant probability P_d. The flying squirrels which could not explore the forest for optimal feed source in late winter and still survived may forage in new directions. It is assumed that only those squirrels that could not search the hickory nuts feed source and still survived will move to different directions in order to find better feed source.

The squirrel searches feed to move away to trees in fixed area (search area) with repeating such processes.

[**SSA algorithm**]

Step 1: Generate equable random locations for *n* number of flying squirrels in allowable search space. Select probability criterions R_1, R_2 and R_3 for searching (0.7 of probability criterions is used in this study case). The number of search is defined as t = 0.

Step 2: Evaluate fitness of each flying squirrel's location $L(x) = \| f(x) - z_0 \|^2$.

Sort the locations of flying squirrels in ascending order depending upon their fitness value.

The flying squirrel with minimal fitness value is supposed on the hickory nut tree x_h^t. The next three best flying squirrels are considered to be on the acorn nut trees x_a^i(i = 1, 2, 3) and they are assumed to move towards hickory nut tree.

The remaining flying squirrels are supposed to be on normal trees x_n^i *(i* = 1,…, *n*-4).

Step 3: Update the position of each flying squirrel as follows:

-Flying squirrels on acorn trees are moving towards hickory nut tree with R_1 of probability

$$x_{a_i}^{t+1} = x_{a_i}^{t} + d_g G_c (x_h - x_{a_i}^{t}), \quad i = 1,2,3 \tag{1}$$

where x_h is the location of flying squirrel that reached hickory nut tree, d_g is random gliding distance and G_c is gliding constant

-Flying squirrels on normal trees are moving towards acorn trees with R_2 of probability.

$$x_{n_i}^{t+1} = x_{n_i}^{t} + d_g G_c (x_{a_j} - x_{n_i}^{t}), \quad i = 1, \cdots, n-4, \tag{2}$$

-Flying squirrels on normal trees are moving towards hickory trees with R_3 of probability.

$$x_{n_i}^{t+1} = x_{n_i}^{t} + d_g G_c (x_h - x_{n_i}^{t}), \quad i = 1, \cdots, n-4, \tag{3}$$

-The rest flying squirrels are moving towards random directions to avoid predator

$$x \sim U(\boldsymbol{D}) \tag{4}$$

where U(D) is equally distributed function in space D.

Step 4: Make seasonal judgment. If the late winter is judged, the positions of the flying squirrels that did not search acorn trees in the past are initialized again.

-Calculate the judgment threshold of the late winter.

$$S_m = S_0 e^{-t/t_m} \tag{5}$$

where S_0-initial threshold, t_m-limitation of time steps.

-When it is late winter, search for the flying squirrels only on normal trees in the past and update their locations.

$$S = \sum_{i=1}^{3} \left\| x_a^i - x_h \right\| \tag{6}$$

If S < S_m, $x_{n_i}^{t} \sim U(\boldsymbol{D}), \boldsymbol{i} \in id$

where *id* means index set of the flying squirrels only on normal trees in the past.

Step 5: If stop condition is not satisfied, go to step 2 with t = t + 1. If stop condition is satisfied, the location of flying squirrel with the lowest fitness value is taken as final optimal solution to finish search process.

The search area D in the algorithm is defined as 4-demention space as follows.

$$D = \prod_{i}^{4} [x_{\min}^{i}, x_{\min}^{i}] \tag{7}$$

where $x_{\min}^{i}$ and $x_{\max}^{i}$ are the upper and lower bounds of range corresponding to measuring date of *i*-th input parameter, respectively.

The generation of random vectors corresponding to x~U(D) are proceeded as follows.

$$x = (x_1, \cdots, x_4)^T \tag{8}$$

$$x_i = x_{\min}^{i} + rand(0,1) \times (x_{\max}^{i} - x_{\min}^{i}) \tag{9}$$

Combined flowchart of neural and SSA is shown in Figure 6.

The method for determining optimal mechanical parameters of coal is presented step by step under the given condition.

4. Case Study

4.1. Determining ranges and levels of back-analysis parameters

The numerical simulations of mechanical model established were conducted with change in mechanical parameters of coal, so that output values simulated from FLAC3D approach approximate range of measured convergence and support load. Mechanical parameters of anthracite coal and host rock of relevant coal mine were measured under the experimental condition, whose value range is shown in Table 2.

Table 2. Mechanical parameters of anthracite coal and host rock.

No.	Rock name	Compressive strength (MPa)	Tensile strength (MPa)	Cohesion (MPa)	Internal friction angle (°)	Elastic modulus (× 10^4 MPa)
1	Anthracite coal	5~13	0.5	1.3~3.1	44	0.5
2	Shale	17-39	3-5	4.2~8.5	15~30	3~5
3	Sandy shale	39-40	4-8	6	30	4~6
4	siltstone	36~56	1~2	17	35~56	2.67

The hanging wall rocks of anthracite coal consist of shale and sandy shale, while footwall rock consists of siltstone. The computational model scope is 60 m in the x-direction, 10 m in y-direction and 65 m in z-direction and coal thickness 5.5 m (Figure 7). There are 28 764 hexahedron elements.

As the studied coal face is buried in 200 m deep from the surface, the vertical distribution load, $P_z = \gamma H = 25000 \times 167.5 = 4\,187\,500\ Pa = 4.185$ MPa is given on the top boundary and lateral distribution load is the same to the vertical distribution load multiplied by 2 (lateral pressure coefficient determined by the field measuring data), that is, $P_x = P_y = \lambda\gamma H = 2 \times 25000 \times 167.5 = 8\,375\,000\ Pa = 8.375\ MPa,$ is given on the both lateral boundaries. Corresponding displacement constrains are given on the rest boundary surfaces of the model, that is, x, y, and z direction displacement of the model bottom are zero and y directional displacements in the front and back plane of the model zero.

The vertical and horizontal distribution loads are given in the interior of model depending on the depth. Material constitutive model is Mohr–Coulomb failure criterion. The material parameters of Mohr–Coulomb failure criterion are volume modulus, shear modulus, cohesion, internal friction angle, dilatant angle and tensile strength. During numerical simulation, only mechanical parameters of coal are changed and properties of host rock remain constant.

In order to consider the interaction between the timber installed in the entry and coal seam around it, vertical distribution reaction is given on the roof, which is distribution load on the timber beam at the moment when the post starts to be driven into the floor coal divided by beam square, that is, 7.056 kN/(2.2×0.18) m^2 = 17.82 kPa. Horizontal distribution reaction is also given on the both sidewalls of entry, whose calculating method is the same above, that is, 28.224 kN/(0.15×2.1) m^2 = 89.6 kPa.

For example, after 6 days lapse of time when the measuring points are installed to determine the ranges and levels of back analyzed parameters of coal consisting of *E*, μ, *C,* and φ, Figures 8-11 show the results of vertical and horizontal convergence of the entry and vertical and horizontal distribution load acting to the timber calculated from FLAC3D.

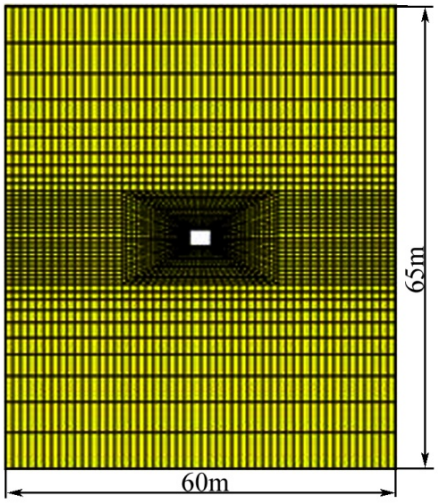

Figure 7. Numerical model.

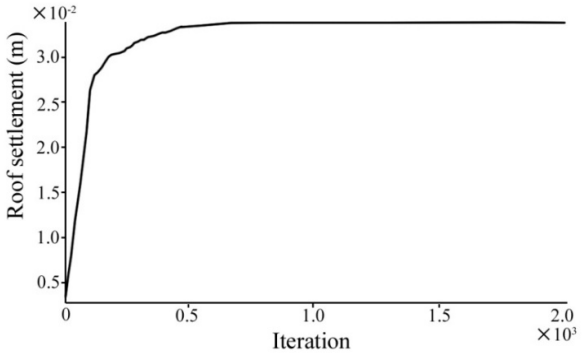

Figure 8. Settle curve of entry roof simulated by FLAC3D after 6 days lapse of time when measurement points are installed.

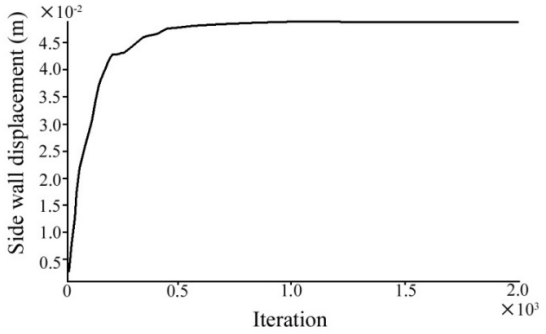

Figure 9. Swelling curve of entry floor simulated by FLAC3D after 6 days lapse of time when measurement points are installed.

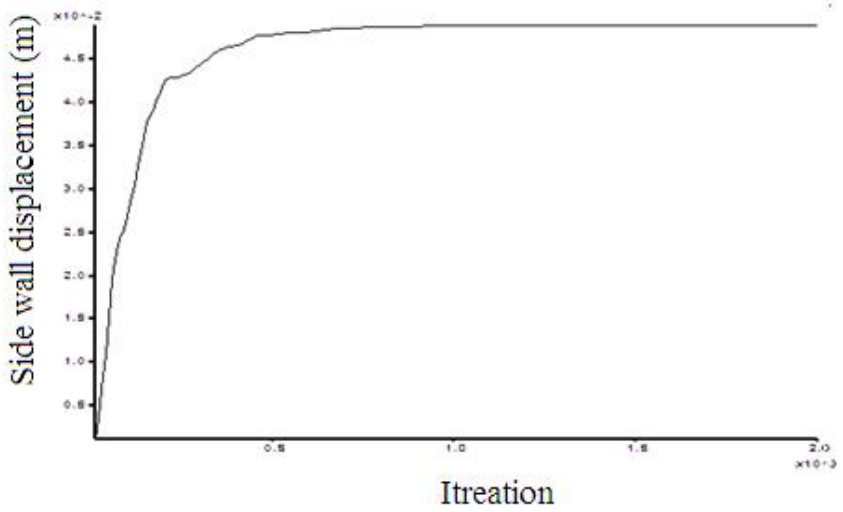

Figure 10. Convergence curve of entry sidewall simulated by FLAC3D after 6 days lapse of time when measurement points are installed.

After 6 days lapse of time when the measuring points are installed, the sum of roof settle and floor swelling of the entry is its convergence, which is 6.5 cm.

After 6 days lapse of time when the measuring points are installed, the convergence of sidewalls of the entry is two times of convergence in its one sidewall , which is 8.4 cm.

After 6 days lapse of time when the measuring points are installed, vertical and horizontal load acting to the timber are the same as the plastic area around the entry multiplied by 19 kN/m^3 of volumetric weight. Table 3 shows initial prediction values of convergences and loads of the entry with measured dates simulated by the above-mentioned method.

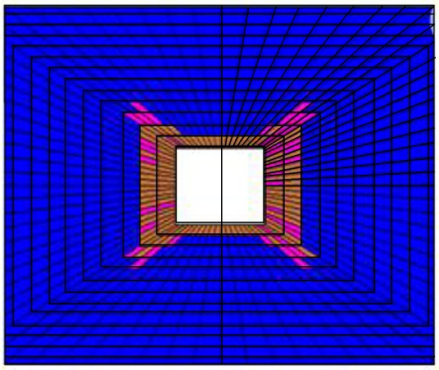

Figure 11. Plastic zone arrounding the entry simulated by FLAC3D after 6 days lapse of time when measurement points are installed.

Table 3. Range of convergences and loads of entry simulated by FLAC3D.

Time (days)	Poisson's ratio	Elastic modulus (MPa)	Lateral pressure coefficient	Cohesion (MPa)	Internal friction angle (°)	Vertical distribution load (KPa)	horizontal distribution load (KPa)	Vertical convergence (m)	Horizontal convergence (m)
3	0.3	499.92	2	4.0	44	3.8	9.5	0.034	0.02
6	0.3	260	2	3.7	42	7.6	15.2	0.065	0.084
9	0.3	129.24	2	3.0	34	51.3	39	0.18	0.294
12	0.3	83.67	2	3.05	35	26.6	34.2	0.22	0.34
15	0.3	51.66	2	3.0	34	29.8	38	0.36	0.57
18	0.3	43.056	2	2.9	33	34.88	47.5	0.41	0.68
21	0.3	41.4	2	2.85	32.6	35.9	58.9	0.42	0.70
24	0.3	39.33	2	2.8	32	41.8	79.8	0.44	0.72

As a result of numerical simulation, the back-analyzed parameters cover the range that the center of Poisson's ratio is 0.3, range of elastic modulus 39.33~499.2MPa, cohesion 2.8~4.0MPa, and internal friction angle 32~44°.

4.2. Elasto–plastic simulation of entry by FLAC3D with orthogonal layout

After setting up the measuring points, elasto–plastic simulation of the entry by FLAC3D was conducted according to the measuring interval. The above-mentioned numerical model, boundary and initial condition remained unchanged and

only mechanical parameters of coal were changed. The levels of the factors for an orthogonal experiment according to the measuring intervals are shown in Table 4.

Table 4. Factor levels of parameters used in FLAC3D simulation according to measuring time.

Measuring interval (days)	Level	Poisson's ratio	Elastic modulus (MPa)	Cohesion (MPa)	Internal friction Angle (°)
3	1	0.31	443.2	3.8	43.5
	2	0.3	499.9	4.0	44
	3	0.29	563.6	4.2[6]	44.5
6	1	0.31	236.77	3.65	41.5
	2	0.3	260	3.7	42
	3	0.29	322	3.75	42.5
…	…	…	…	…	…
24	1	0.32	36.18	2.79	31.8
	2	0.31	39.33	2.8	32
	3	0.29	44.8	2.81	32.2

Numerical simulations were conducted by FLAC3D according to the orthogonal experiment layout with factor levels shown in Table 4 and orthogonal experiment layout and numerical simulation results are shown in Table 5. Here, A means Poisson's ratio, B elastic modulus, C cohesion, and D internal friction angle in Table 5. Orthogonal experiment layout $L_{12}(4^3)$ was used to consider the mixed effect of several parameters and numerical simulations were conducted to change mechanical parameters of corresponding levels. Generally, we conducted numerical simulations numbered 96.

4.3. Relation model between mechanical parameters of coal and supposed load and convergence by hierarchical neural network

The relation between input and output of the hierarchical neural network is as follows.

$$\begin{cases} u_j^k = \sum_{i=1}^{n_{k-1}} w_{ji}^k z_i^{k-1} + h_j^k \\ z_j^k = f_j^k(u_j^k) \quad (k=\overline{1, L}, j=\overline{1, n_k}) \end{cases} \tag{10}$$

where n is number of input signals of neural network, p is the number of output signals of neural network, n_k is the number of neurons in the k-th layer, L–number of layers of neural network, $x_i = z_i^0 \quad (i=\overline{1,n})$ is i-th input signal of neural network, $\boldsymbol{x}=(x_1, x_2, \ldots, x_n)^T$ is the input signal vector of neural network, $z_j = z_j^L (j=\overline{1, p})$ is the output signal of j-th neuron of neural network, $\boldsymbol{z}=(z_1, z_2, \ldots, z_p)^T$ is the output signal vector of neural network, $z_j^k (j=\overline{1, n_k})$ is the output signal of j-th neuron in the k-th layer, $u_j^k (j=\overline{1, n_k})$ is the internal potential signal of j-th neuron in the k-th layer, w_{ji}^k is the combined weight of i-th neuron in the k-1-th layer, and j-th neuron in the k-th layer, h_j^k is bias value of j-th neuron in the k-th layer, and $f_j^k (j=\overline{1, n_k})$ is the output function of j-th neuron in the k-th layer.

In this study, the input vector $\boldsymbol{x}=(x_1, x_2, \ldots, x_4)^T$ consists of E, μ, C, and φ and output vector $\boldsymbol{z} = (z_1, z_2, \ldots, z_4)^T$ is two convergence displacements and two loads acting on the timber.

Detailed structure parameters of the neural network are listed in Table 6.

Table 5. Orthogonal layout $L_{12}(4^3)$ and values simulated by FLAC3D.

Measuring interval (days)	Simulation plan	Factors							
		A	B	C	D	Vertical Load (kPa)	Horizontal load (kPa)	Vertical convergence (m)	Horizontal convergence (m)
3	1	1	1	1	1	5.7	13.3	0.034	0.051
	2	1	2	2	2	5.7	11.4	0.034	0.05
	3	1	3	3	3	5.7	13.3	0.032	0.048
	4	2	1	1	2	5.7	15.2	0.034	0.05
	5	2	2	2	3	5.7	15.2	0.0324	0.049
	6	2	3	3	1	5.7	13.3	0.031	0.0314
	7	3	1	1	1	5.7	17.1	0.032	0.05
	8	3	2	2	2	5.7	15.2	0.0314	0.048
	9	3	3	3	3	3.8	13.3	0.0308	0.046
	10	1	1	3	3	5.7	13.3	0.034	0.07
	11	1	2	1	1	7.6	17.1	0.0332	0.0332
	12	1	3	2	2	5.7	15.2	0.0328	0.0488
6	1	1	1	1	1	7.6	19	0.072	0.0104
	2	1	2	2	2	7.6	19	0.064	0.1004
	3	1	3	3	3	7.6	17.1	0.068	0.097
	4	2	1	1	2	7.6	19	0.066	0.103
	5	2	2	2	3	7.6	19	0.064	0.10
	6	2	3	3	1	7.6	20.9	0.064	0.097
	7	3	1	1	1	7.6	19	0.066	0.103
	8	3	2	2	2	5.7	17.1	0.0634	0.099
	9	3	3	3	3	5.7	19	0.062	0.095
	10	1	1	3	3	5.7	19	0.0664	0.104
	11	1	2	1	1	7.6	19	0.065	0.102
	12	1	3	2	2	7.6	19	0.064	0.098
…	…	…	…	…	…	…	…	…	…
24	1	1	1	1	1	53.2	84.4	0.454	0.76
	2	1	2	2	2	53.2	83.6	0.44	0.72
	3	1	3	3	3	51.3	72.2	0.441	0.70
	4	2	1	1	2	49.4	85.5	0.452	0.76
	5	2	2	2	3	49.4	77.9	0.432	0.72
	6	2	3	3	1	52.3	83.6	0.42	0.70
	7	3	1	1	1	49.4	89.8	0.45	0.76
	8	3	2	2	2	49.4	83.6	0.43	0.72
	9	3	3	3	3	47.5	74.1	0.44	0.69
	10	1	1	3	3	45.6	74.1	0.46	0.766
	11	1	2	1	1	55.1	83.9	0.44	0.71
	12	1	3	2	2	53.2	83.6	0.43	0.70

Table 6. Characteristics of BP neural network.

Index	Value
Number of input neurons	4
Number of output neurons	4
Number of hidden layer	1
Number of neurons in the hidden layer	30
Transfer function of hidden layer	tansig
Learning error	10^{-5}

The basic skills for establishing the optimal neural network architecture is to search for number of hidden layers and number of neurons in each layer. The optimal neural network structure searched through several tens of training is 4-30-4 based on engineering experience and judgment, whose learning error curve is shown in Figure 12.

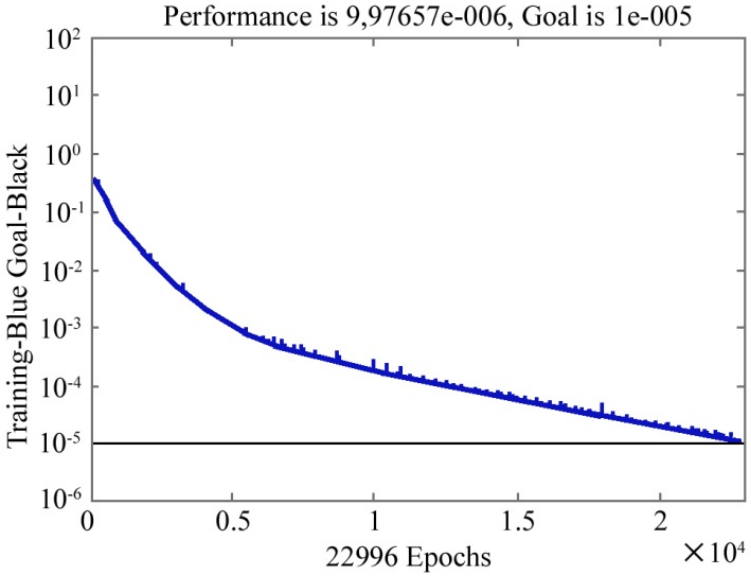

Figure 12. Error convergence curve of neural network learning.

The weights and biases between input layer and hidden layer, hidden layer, and output layer are searched through the neural network training. The maximum relative error is less than 3% from testing result on the back-propagation neural network structure established.

The non-linear relation $z = f(x)$ between the input parameters and output values according to the measured intervals of 3 days, 6 days, 9 days,..., 24 days from the start of measurement are established by using the above-mentioned method to make the database for combining operation with SSA algorithm.

Non-linear relation equation $z = f(x)$ is composed in detail as follows:

$$\begin{cases} z_1 = \tan sig\,(W_1 x + h_1) \\ z = W_2 z_1 + h_2 \end{cases} \quad (11)$$

That is:

$$z = f(x) = W_2\left[\tan sig\,(W_1 x + h_1)\right] + h_2 \quad (12)$$

where W_1 and W_2 are weight vector of 4 × 4 matrix type, respectively. h_1 and h_2 are bias vector of 4 × 1 matrix type, respectively. x is input vector of 4 × 1 matrix type. z_1 is hidden output vector of 4 × 1 matrix type. z is output vector of 4 × 1 matrix type.

If input vector $x = (x_1, x_2, \ldots, x_4)^T$, that is Poisson's ratio, elastic modulus, cohesion, and internal friction angle of anthracite coal are given, output vector $z = (z_1, z_2, \ldots, z_4)^T$, that is vertical and horizontal distribution load on the timber and vertical and horizontal convergence of entry can be solved from Eq. (12). Therefore, mechanical parameters of coal can be determined from the above function relation.

5. Results and Discussion

Under the condition that the relation between mechanical parameters of coal and the displacements and loads on timber are given through the neural network training, mechanical parameters of coal corresponding to the measured displacement and load on the timber z_0 refers to the problem for solving x_0 satisfying $z_0 = f(x_0)$ from $z = f(x)$ with sufficient correctness.

This problem can be solved as following optimal problem:

$$x_0 = \underset{x \in D}{argmin} \left\| f(x) - z_0 \right\|^2 \quad (13)$$

Figure 13 shows the combined flowchart of ANN and SSA proposed in this paper in more detail.

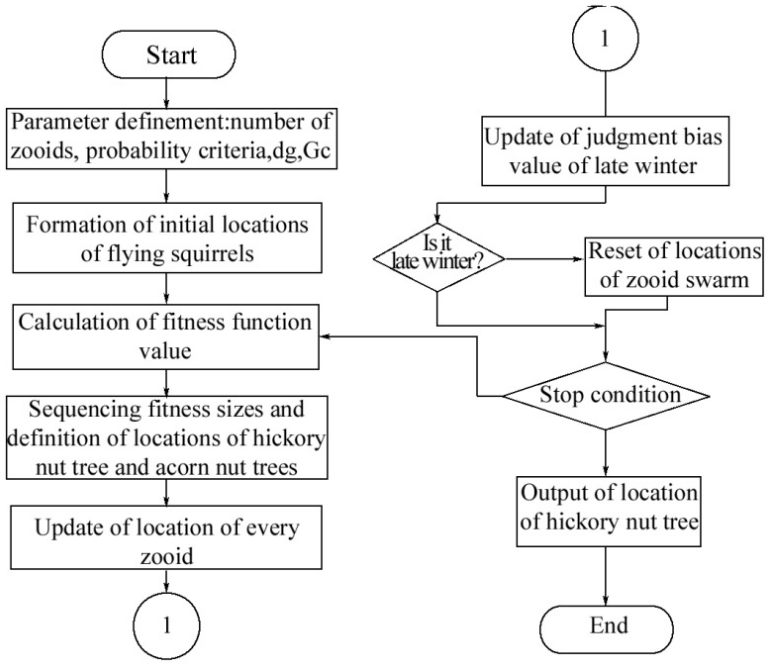

Figure 13. SSA search flowchart combined with ANN.

For example, when input parameter values and measured values corresponding to 3 days after installing the measuring points (that is, vertical and horizontal distribution load acting to the timber and vertical and horizontal convergence of the entry) are substituted into SSA to conduct searching operation, obtained convergence curve of fitness function is shown in Figure 14. The changing characteristics of mechanical parameters predicted from the SSA are given in Table 7 according to the measuring interval.

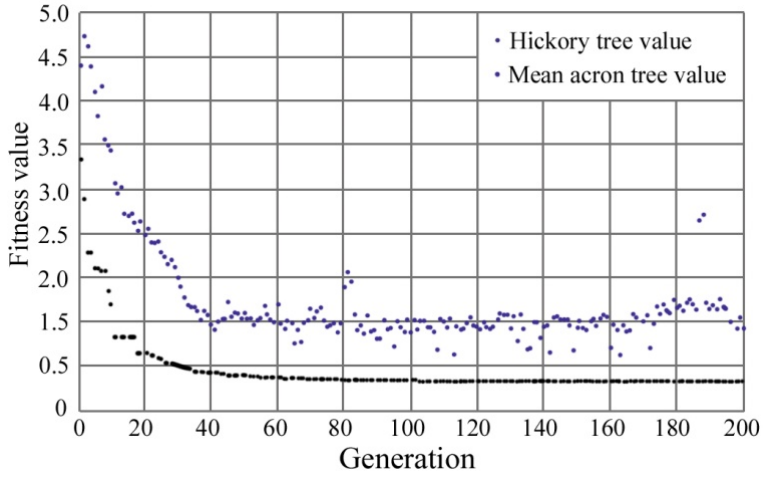

Figure 14. Convergence curve of fitness function according to generations.

Table 7. Optimal values of mechanical parameters of anthracite coal estimated form SSA.

Time (day)	Fitness function	Poisson's ratio	E (MPa)	C (MPa)	φ (°)
3	0.3545	0.308499	563.541	4.19894	44.4796
6	13.5361	0.291138	321.974	3.73667	41.5066
9	33.9152	0.30508	148.267	3.34982	37.0005
12	86.0943	0.295423	71.7582	3.00389	35.1152
15	121.0306	0.304686	48.0516	3.04995	33.5006
18	143.2855	0.310126	47.6557	2.86503	32.8495
21	178.8186	0.314098	43.8695	2.81458	32.708
24	216.7034	0.29389	43.4604	2.80998	31.8002

To verify the good performance of new combination of the ANN and SSA, the comparison studies between back analysis method by ANN-SSA and those by ANN-PSO [22] and ANN-GA [20] with same purpose are conducted using data measured in coal face entry of Sinchang coal mine (Figures 4 and 5) as an example. As the verification is performance estimation of optimization methods, modeling method of vertical and horizontal load and vertical and horizontal convergence of coal face entry by ANN does not change and the optimization of Eq. (13) on model function is conducted using above three intelligent back-analysis methods. This time, parameters in every method are established in Table 8 according to literatures [22].

The errors of measured values (Figures 4 and 5) and back-estimation values by ANN-SSA, ANN-PSO, and ANN-GA are as follows depending on time (3-24 days).

Table 8. Established values of simulation parameters.

GA parameter	Value
Size of population	50
Rate of mutation	0.05
Rate of cross-over	0.7
PSO parameter	Value
Size of population	50
W	0.5
C1	2
C2	2
SSA parameter	Value
Size of population	50
G_c	1.9
R_i	0.7
d_g	2
t_m	50

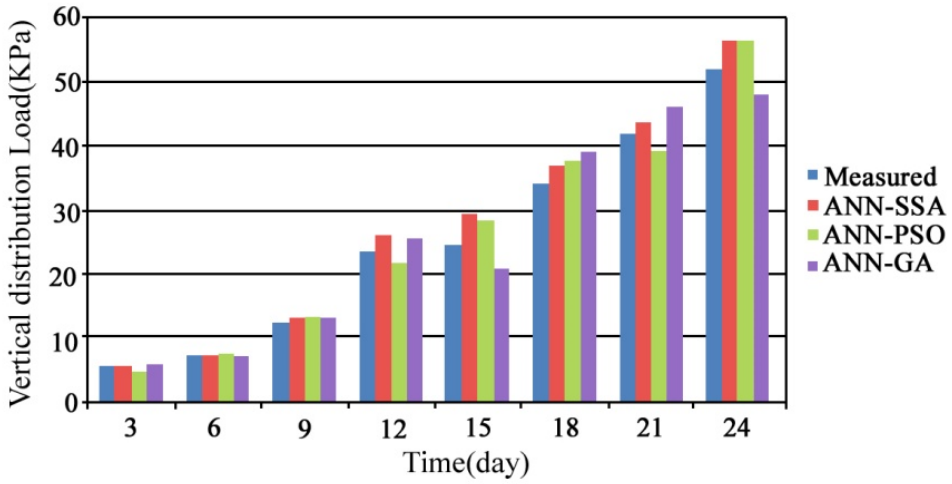

Figure 15. Comparison between measured vertical distribution load acting to the timber and values estimated by ANN-SSA, ANN-PSO, and ANN-GA.

Table 9. Absolute errors of estimated vertical load (unit: kPa).

Dates	ANN-SSP	ANN-PSO	ANN-GA
3	0.05	0.82	0.13
6	0.09	0.13	0.21
9	0.7	0.8	0.78
12	2.5	1.8	2.1
15	4.7	3.9	3.8
18	2.9	3.5	4.9
21	1.8	2.9	3.8
24	4.3	4.2	4.3
Mean	2.13	2.25625	2.5025

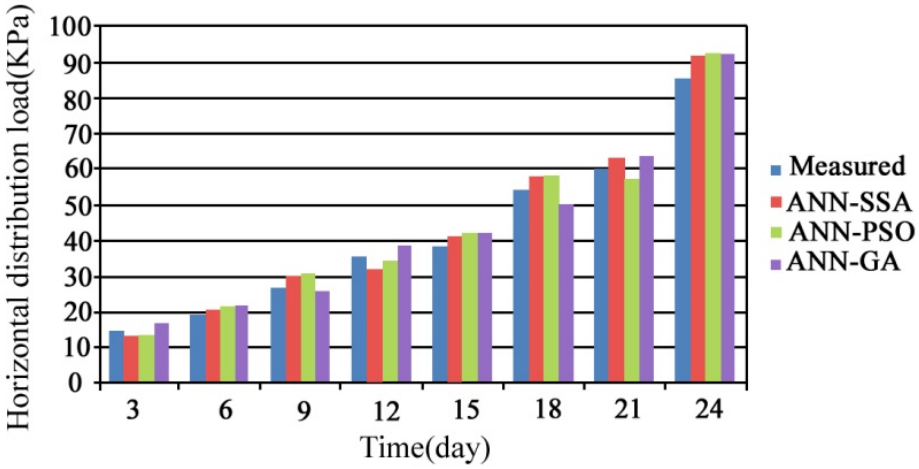

Figure 16. Comparison between measured horizontal distribution load acting to the timber and values estimated by ANN-SSA, ANN-PSO and ANN-GA.

Table 10. Absolute errors of estimated horizontal load (unit: kPa).

Dates	ANN-SSP	ANN-PSO	ANN-GA
3	1.3	1.3	2.3
6	1.6	2.6	2.7
9	3.3	3.9	1.1
12	3.6	1.6	3.4
15	3.2	3.6	3.9
18	3.7	3.9	4.1
21	2.7	2.9	3.1
24	6.4	6.8	7.1
Mean	3.225	3.325	3.4625

As shown in Figures 15 and 16 and Tables 9 and 10, the mean absolute errors between the vertical and horizontal distribution load and predicted values from the method proposed in this paper are very small, which are 2.13 kPa and 3.225 kPa, respectively. However, the mean relative errors between the values predicted in accordance with ANN-GA, ANN-PSO and measured values are larger than 2.25 kPa and 3.3 kPa, respectively.

Therefore, the vertical and horizontal distribution load predicted from ANN-SSA is revealed to be in good agreement with the corresponding measured vertical and horizontal distribution load.

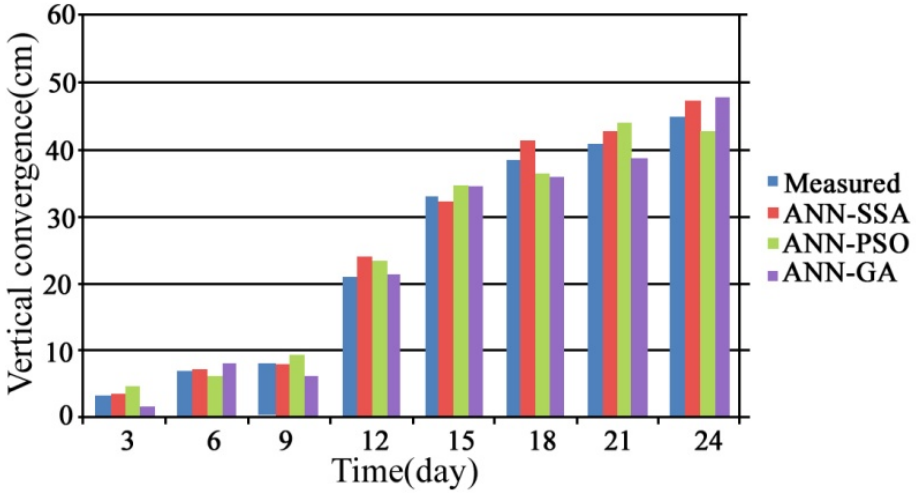

Figure 17. Comparison between vertical convergence measured in entry and values estimated by ANN-SSA, ANN-PSO and ANN-GA.

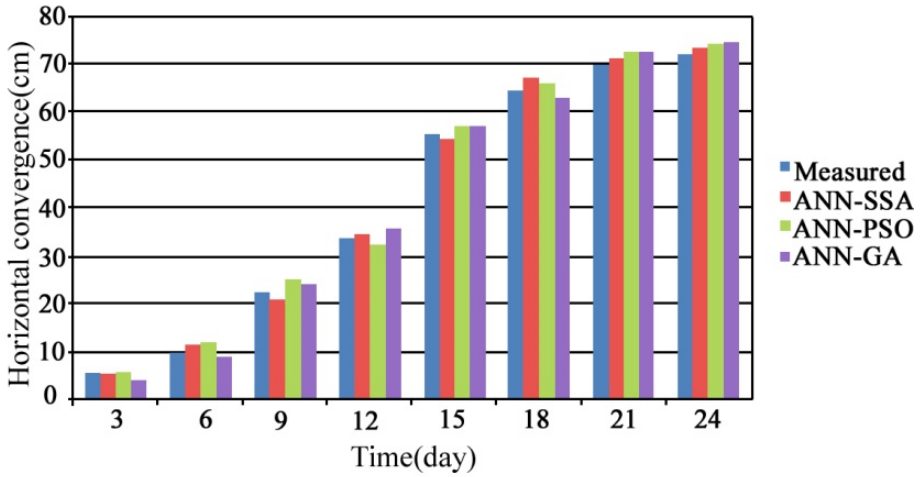

Figure 18. Comparison between horizontal convergence measured in entry and values estimated by ANN-SSA, ANN-PSO and ANN-GA.

Table 11. Absolute errors of estimated vertical convergence (unit: cm).

Date	ANN-SSP	ANN-PSO	ANN-GA
3	0.09	1.2	1.8
6	0.2	0.8	1.2
9	0.4	1.2	1.8
12	3.1	2.5	0.3
15	0.9	1.3	1.3
18	3	2.1	2.3
21	2.1	3.2	1.9
24	2.4	2.1	3.1
Mean	**1.52375**	**1.8**	**1.7125**

Table 12. Absolute errors of estimated horizontal convergence (unit: cm).

Date	ANN-SSP	ANN-PSO	ANN-GA
3	0.1	0.15	1.3
6	1.27	1.91	1.17
9	1.5	2.5	1.9
12	0.9	1.3	1.9
15	1.4	1.3	1.4
18	2.6	1.6	1.6
21	1.7	2.7	2.7
24	1.3	1.9	2.3
Mean	1.34625	1.67	1.78375

As shown in Figures 17 and 18 and Tables 11 and 12, the mean absolute errors between the vertical and horizontal convergence and values predicted from ANN-SSA are very small and maximum relative error is less than 1.53 cm and 1.346 cm, respectively. However, the mean absolute errors between the values predicted in accordance with ANN-GA and ANN-PSO and measured values are less than 1.7 cm and 1.6 cm, respectively. Therefore, the vertical and horizontal convergence predicted from ANN-SSA is revealed to be in good agreement with the corresponding

measured vertical and horizontal convergence.

As shown in the above figures and tables, ANN-SSA method proposed in this paper is relatively smaller in view of the mean absolute error. As the absolute errors between measured values and back-estimated values become larger with the increase of measurement days (3-24 days), the mean absolute error (MAE) of weighted error norm of Eq. (13) is selected as the comprehensive comparison standard.

$$MAE = \frac{1}{N}\sum_{t=1}^{N}\left\| z_{meas} - z_{pred} \right\| W_t \qquad (14)$$

where W_t –weighted value about covariance matrix of vertical and horizontal load and vertical and horizontal convergence simulated according to Table 5.

As shown in the Table 13, MAE of ANN-SSA is relatively smaller in comparison with other methods.

It can be seen that the mechanical parameters of rock mass around the drifts or chambers driven in soft rock seam can be predicted with high accuracy by the method proposed in this paper. The elastic modulus, cohesion and internal friction angle of anthracite coal depending on time are shown in Figures 19, 20, and 21.

Table 13. MAE according to methods.

No	Method	MAE
1	ANN-SSA	2.49
2	ANN-PSO	3.12
3	ANN-GA	3.68

As shown in Figure 19, it can be seen the elastic modulus of anthracite coal predicted from ANN-SSA decreased depending on time, especially, rapidly drops for 12 days after driving entry and installing timbers and slowly after 12 days. This is agreed with the tendency that vertical and horizontal displacement measured from the field continuously increase. It is also predicted that anthracite coal surrounding the entry nearly failed after 12 days.

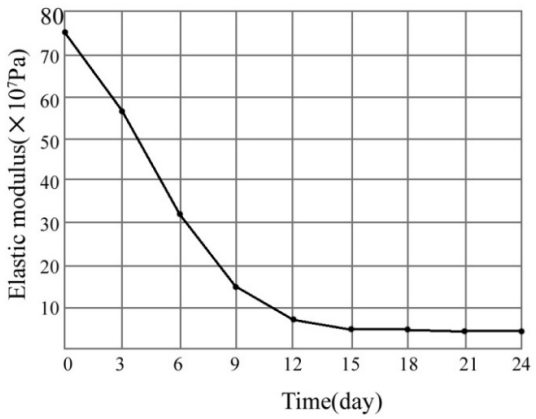

Figure 19. Change of the elastic modulus of anthracite coal depending on time.

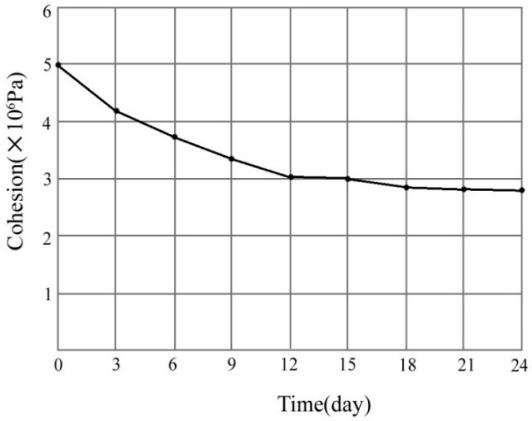

Figure 20. Change of the cohesion of anthracite coal depending on time.

As shown in Figure 20, it can be seen that the cohesion of anthracite coal predicted from ANN-SSA decreased depending on time, especially, rapidly drops for 12 days after driving entry and installing timbers and slowly after 12 days. This is agreed with the tendency that vertical and horizontal load measured from the field continuously increase. It is also proved that anthracite coal surrounding the entry nearly failed after 12 days. Therefore, we can predict that whole weight of coal upper the beam and leg of wooden timer acts to them depending on time.

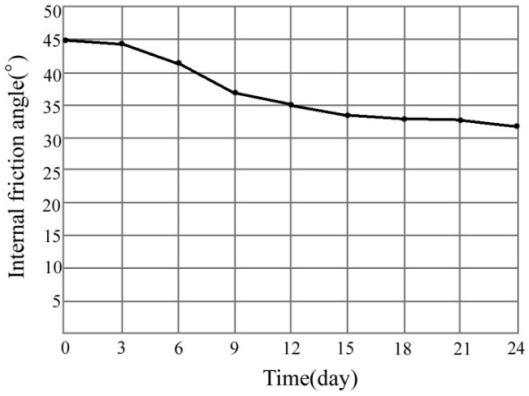

Figure 21. Change of the internal friction angle of anthracite coal depending on time.

As shown in Figure 21, it can be seen that the internal angle of anthracite coal predicted from ANN-SSA also decreased slowly with time. It is proved that the internal angle of anthracite coal has considerable influence the weakening of coal strength.

Therefore, the vertical and horizontal distribution load and vertical and horizontal displacement predicted from ANN-SSA are revealed to be in good agreement with the corresponding data measured from field, which has validated that the accuracy and reliability of depending-time mechanical parameters of anthracite coal and ANN-SSA proposed in this paper.

6. Conclusions

The aim of this work was to assess effectiveness of new combination of ANN and SSA back-analysis of time-depending mechanical parameters of anthracite coal based on timber loads and displacements measured in the coal face entry. For this, we proposed the methodology that could predict the time-depending coal mechanical parameters by the combination of FLAC3D numerical simulation based on measured load and displacement, establishment of three layers BPNN and SSA.

The main results of this study are as follows:

1. The study clarified the reason why rock pressure of the entry driven in the anthracite coal seam was very severely through the in situ observation and measurement.

2. This paper proposed the methodology for back-analyzing the mechanical parameters of anthracite coal by using the combination of FDM with ANN and SSA, which can make clear the rock pressure phenomena of the entry that are very difficult to illustrate this process analytically and by other back analysis methods.

Based on an FDM computation using the back-analyzed optimal mechanical parameters, the displacements and support loads for all monitoring points of the multi-point displacement measurement were computed and found to exhibit good agreement with the measured values. The method developed in this study can provide a useful basis for predicting time-dependent behavior of medium surround the drift or chamber driven in such soft rock as the anthracite coal. Future work will address the comprehensive consideration of time-dependent mechanical characteristics of coal seam, hanging wall and footwall rock seam to measure rational entry maintenance.

Data Availability

The data used to support the findings of this study is available from the corresponding author upon request.

Conflicts of Interest

The authors declare that they have no conflicts of interest regarding the publication of this paper.

Acknowledgment

This work was supported by the National Science and Technical Development Foundation of DPR Korea (Grant No. 24-21630312).

References

[1]. Shang, Y.J., Cai, J.G., Hao, W.D., Wu, X.Y., and Li, S.H. (2002). Intelligent back analysis of displacements using precedent type analysis for tunnelling. Tunnelling and Underground Space Technology, 17: 381–389.

[2]. Sakurai, S. and Takeuchi, K. (1983). Back-analysis of measured displacement of tunnels. Rock Mechanics and Rock Engineering, 16: 173–180.

[3]. Oreste, P. (2005). Back-analysis techniques for the improvement of the understanding of rock in underground constructions. Tunnelling and Underground Space Technology, 20: 7–21.

[4]. Han, U.C., Choe, C.S., Hong, K.U., and Han, H.I. (2021). Intelligent back-analysis of geotechnical parameters for time-dependent rock mass surrounding mine openings using grey Verhulst model. Journal of Central South University, 28: 3099-3116.

[5]. Kaiser, P.K., Zou, D. P., and Lang, A. (1990). Stress determination by back analysis of excavation-induced stress changes: a case study. Rock Mechanics and Rock Engineering, 23: 185–200.

[6]. Li, F., Wang, J., and Brigham, J.C. (2014) Inverse calculation of in situ stress in rock mass using the surrogate-model accelerated random search algorithm. Computers and Geotechnics, 61: 24–32.

[7]. Ghorbani, M. and Sharifzadeh, M. (2009). Long term stability assessment of Siah Bisheh powerhouse cavern based on displacement back-analysis method. Tunnelling and Underground Space Technology, 24: 574–583.

[8]. Zhang, L.Q., Yue, Z.Q., Yang, Z.F., Qi, J.X., and Liu, F.C. (2006). A displacement- based back-analysis method for rock mass modulus and horizontal in situ stress in tunnelling-illustrated with a case study. Tunnelling and Underground Space Technology, 21: 636–649.

[9]. Hisatake, M. and Hieda, Y. (2008). Three-dimensional back-analysis method for the mechanical

parameters of the new ground ahead of a tunnel face. Tunnelling and Underground Space Technology, 23: 373–380.

[10]. Yang, L., Zhang, K., and Wang, Y. (1996). Back analysis of initial rock time-dependent parameters. International Journal of Rock Mechanics and Mining Sciences & Geomechanics Abstracts, 33(6): 641-645.

[11]. Liang, Y.C., Feng, D.P., Liu, G.R., Yang, X.W., and Han, X. (2003). Neural identification of rock parameters using fuzzy adaptive learning parameters. Computers & Structures, 81: 2373–2382.

[12]. Feng, X.-T., Zhao, H., and Li, S. (2004). A new displacement back analysis to identify mechanical geo-material parameters based on hybrid intelligent methodology. International Journal for Numerical and Analytical Methods in Geomechanics, 28: 1141–65.

[13]. Feng, X.-T., Zhang, Z., and Sheng, Q. (2000). Estimating mechanical rock mass parameters relating to the Three Gorges Project permanent shiplock using an intelligent displacement back analysis method," International Journal of Rock Mechanics and Mining Sciences, 37(7): 1039-1054.

[14]. Yu, Y., Zhang, B., and Yuan, H. (2007). An intelligent displacement back-analysis method for earth-rockfill dams. Computers and Geotechnics, 34: 423–434.

[15]. Zhang, L.Q., Yue, Z.Q., Yang, Z.F., Qi, J.X., and Liu, F.C. (2006). A displacement-based back-analysis method for rock mass modulus and horizontal in situ stress in tunneling – Illustrated with a case study. Tunnelling and Underground Space Technology, 21: 636–649.

[16]. Yazdani, M., Sharifzadeh, M., Kamrani, K., and Ghorbani, M. (2012). Displacement-based numerical back analysis for estimation of rock mass parameters in Siah Bisheh powerhouse cavern using continuum and discontinuum approach. Tunnelling and Underground Space Technology, 28: 41–48.

[17]. Sharifzadeh, M., Tarifard, A., and Moridi, M.A. (2013). Time-dependent behaviour of tunnel lining in weak rock mass based on displacement back-analysis method," Tunnelling and Underground Space Technology, 38: 348–356.

[18]. Gao, W. and Ge, M. (2016). Back-analysis of rock mass parameters and initial stress for the Longtan tunnel in China. Engineering with Computers, 32: 497–515.

[19]. Yu, F., Peng, X., and Su, L. (2017). A back-propagation neural-network-based displacement back analysis for the identification of the geo-mechanical parameters of the Yonglang landslide in China. Journal of Mountain Science, 14: 1739–1750.

[20]. Gao, W., Chen, D., Dai, S., and Wang, X. (2018). Back-analysis for mechanical parameters of surrounding rock for underground roadways based on new neural network. Engineering with Computers, 34: 25–36.

[21]. Luo, Y., Chen, J., Chen, Y., Diao, P., and Qiao, X. (2018). Longitudinal deformation profile of a tunnel in weak rock mass by using the back analysis method. Tunnelling and Underground Space Technology, 71: 478-493.

[22]. Mohamad, T., Armaghani, E. J., and Moment, D. (2015). Prediction of the unconfined compressive strength of soft rocks: a PSO-based ANN approach. Bulletin of Engineering Geology and the Environment, 74(3): 745-757.

[23]. Rezaei, M. (2020). Predicting Unconfined Compressive Strength of Intact Rock using New Hybrid Intelligent Models. Journal of Mining and Environment, 11: 231-246.

[24]. Rezaei, M. (2022). Feasibility of novel techniques to predict the elastic modulus of rocks based on the laboratory data. International Journal of Geotechnical Engineering, 14: 25-34.

[25]. Rezaei, M. (2018). Indirect measurement of the elastic modulus of intact rock using the Mamdani fuzzy inference system. Measurement, 129: 319-331.

[26]. Wang, Y. and Rezaei, M. (2023). Developing Two Hybrid Algorithms for predicting the elastic modulus of intact rocks. Sustainability, 15: 1-24.

[27]. Jain, M., Singh, V., and Rani, A. (2019). A novel nature-inspired algorithm for optimization: Squirrel search algorithm. Swarm and Evolutionary Computation, 44: 148-175.

تعیین پارامترهای مکانیکی زغال سنگ آنتراسیت با استفاده از الگوریتم جستجوی سنجاب پرنده با داده های بار و جابجایی لارده چوبی

میونگ نام سین [۱]، اون چول هان [۲*]، هیون هیوک ری [۱]، و سونگ ایل جون [۳]

۱. دانشکده مهندسی معدن، دانشگاه صنعتی کیم چاک، پیونگ یانگ، جمهوری دموکراتیک خلق کره
۲. دانشکده علوم و مهندسی، دانشگاه صنعتی کیم چاک، پیونگ یانگ، جمهوری دموکراتیک خلق کره
۳. گروه ریاضیات کاربردی، دانشگاه صنعتی کیم چاک، پیونگ یانگ، جمهوری دموکراتیک خلق کره

ارسال ۲۰۲۳/۰۳/۲۲، پذیرش ۲۰۲۳/۰۵/۰۴

* نویسنده مسئول مکاتبات: huch8272@star-co.net.kp

چکیده:

لایه زغالسنگ آنتراسیت جمهوری دموکراتیک خلق کره به دلیل اقدامات زمین ساختی و زمین شناسی در چندین مرحله در دوران مزوزوئیک به ذرات تبدیل شد تا نرم شود. از آنجایی که چین‌ها و گسل‌ها بیش از حد توسعه یافته‌اند و شکل لایه زغالسنگ بسیار پیچیده است، استخراج زغالسنگ آنتراسیت توسط سیستم استخراج جبهه‌کار طولانی غیرممکن است و زغالسنگ عمدتاً توسط سیستم استخراج تخریبی استخراج شده است. هدف از این کار ارزیابی اثربخشی ترکیب جدید الگوریتم جستجوی سنجاب پرنده (SSA) و شبکه عصبی مصنوعی (ANN) برای تجزیه و تحلیل برگشتی پارامترهای مکانیکی وابسته به زمان زغالسنگ آنتراسیت بر اساس بارهای وارده بر پایه‌های چوبی و جابجایی اندازه‌گیری شده در جبهه‌کار زغالسنگ است. مطالعه موردی به یک ورودی جبهه‌کار زغالسنگ در معدن زغالسنگ Sinchang واقع در شهرستان Unsan، استان پیونگان جنوبی، DPR کره می‌پردازد. برای تأیید عملکرد خوب ترکیب جدید SSA و ANN، مطالعات مقایسه‌ای بین روش تحلیل برگشتی پیشنهادی و روش‌های دیگر با همین هدف، با استفاده از داده‌های اندازه‌گیری شده در ورودی جبهه‌کار زغالسنگ انجام می‌شود. میانگین خطای مطلق (MAE) هنجار خطای وزنی ANN-SSA در مقایسه با سایر روش‌ها نسبتاً کوچکتر است که ۲.۴۹ است. تحلیل برگشتی جدید روش خوبی برای تعیین پارامترهای مکانیکی وابسته به زمان مناسب زغالسنگ آنتراسیت در اطراف ورودی در لایه زغالسنگ بسیار نرم است.

کلمات کلیدی: SSA، تحلیل برگشت جابجایی، شبکه عصبی، پارامتر مکانیکی وابسته به زمان.